

## Inducing Photonic Transitions between Discrete Modes in a Silicon Optical Microcavity

Po Dong, Stefan F. Preble, Jacob T. Robinson, Sasikanth Manipatruni, and Michal Lipson\*

*School of Electrical and Computer Engineering, Cornell University, Ithaca, New York 14853, USA*

(Received 13 September 2007; revised manuscript received 20 November 2007; published 25 January 2008)

We show the existence of direct photonic transitions between modes of a silicon optical microcavity spaced apart in wavelength by over 8 nm. This is achieved by using ultrafast tuning of the refractive index of the cavity over a time interval that is comparable to the inverse of the frequency separation of modes. The demonstrated frequency mixing effect, i.e., the transitions between the modes, would enable on-chip silicon comb sources which can find wide applications in optical sensing, precise spectroscopy, and wavelength-division multiplexing for optical communications and interconnects.

DOI: [10.1103/PhysRevLett.100.033904](https://doi.org/10.1103/PhysRevLett.100.033904)

PACS numbers: 42.82.-m, 42.60.Da, 42.72.-g, 42.79.Nv

With advances in nanotechnology, optical microcavities [1,2] have recently enabled optical functional devices which achieve strong light-matter interactions by high confinement of light [3–7]. The modes of an optical cavity are quantized, their separation in frequency being inversionally proportional to the size of the cavity. It has been shown recently that if a cavity is tuned while light is trapped in the resonator, i.e., in a time scale shorter than the photon lifetime, the properties of light, such as bandwidth and wavelength will follow the properties of the cavity [8–11]. In these works, however, the modes of the cavity remain independent, i.e., light propagates in only one of the modes of the (tuned) cavity. When light is trapped in the cavity and the cavity's refractive index is tuned quickly enough, not only relative to the photon lifetime but also relative to the inverse of the frequency spacing of the cavity's modes, it is possible to induce photonic transitions between the modes of the cavity. Transitions between optical modes were previously observed using a modulator in large optical cavities, for example, in frequency comb generators [12] and mode-locked lasers [13]; however, the spacing between the modes is usually small, typically less than 50 GHz. Here in contrast we show the effect for the first time in ultracompact cavities in which the modes are very far from each other, approximately 1 order of magnitude farther in wavelength than in previously demonstrated macroscopic systems. We induce the transitions using an ultrafast modulation of the cavity's refractive index that in the frequency domain overlaps with more than 15 modes of the compact structure.

In this work the optical microcavity is realized using a silicon-on-insulator ring resonator with a 450-nm-wide by 250-nm-high rectangular cross section. The ring is coupled to two straight waveguides, one acting as an input port, and the other acting as a drop port, as seen in the inset of Fig. 1. The optical resonance condition is satisfied when the circumference of the ring corresponds to an integer multiple of guided wavelengths. Under this condition the light is strongly localized in the ring and collected by the drop waveguide. The quasi-TM transmission spectrum shows

that the free spectral range of this ring is 0.82 nm at a wavelength of 1540 nm for a ring resonator with a 100  $\mu\text{m}$  radius. Here we use a relatively large ring to show the transition between a large number of modes due to the small free spectral range in the structure. We use the free-carrier plasma dispersion effect [14] to produce an ultrafast change in the refractive index of the ring resonator. The free carriers are generated by illuminating the top of the ring with a femtosecond pulsed laser (the pulse duration is 200 fs) centered at a wavelength of 412 nm and a repetition

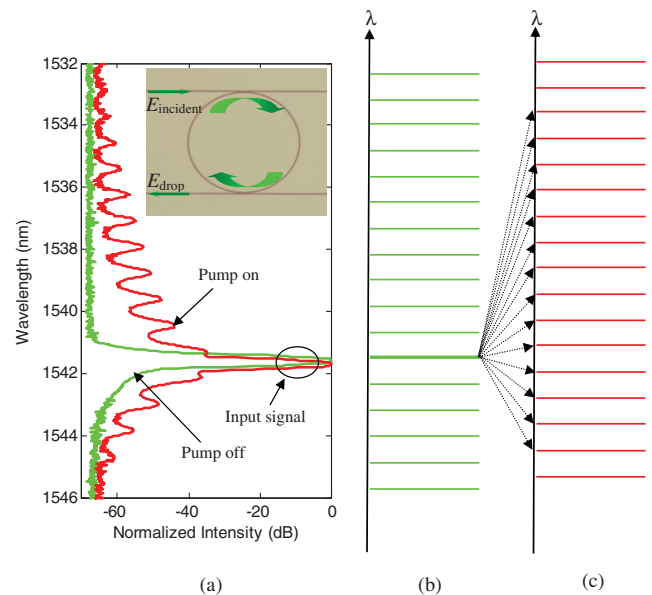


FIG. 1 (color). (a) Spectrum of the drop port measured for a ring resonator with a radius 100  $\mu\text{m}$ . A band-pass filter is used to eliminate amplified spontaneous emission of the input probe laser. The green line shows the reference spectrum when pump is off, and the probe beam is on resonance. The red line shows the spectrum following the pump pulse where 15 new wavelengths are generated simultaneously. Inset, the top-view microscope image of the fabricated device. (b),(c) The diagram of the discrete cavity modes of an optical microcavity before (b) and after (c) pump is incident on the sample.

rate of 76 MHz [15]. At this wavelength the laser is strongly absorbed by the silicon layer and free electron-hole pairs are generated in a time approximately equal to the pulse duration of the pump, which is much smaller than the photon lifetime of the cavity. The generated electron-hole pairs modify the dielectric function of the cavity [14]. Thereafter, they are subjected to dynamic recombination processes on a time scale of  $\sim 450$  ps [15]. A continuous-wave (cw) laser provides the probe signal, which is confined in the ring resonator and then is converted to new frequencies by the pump induced dynamic change in the cavity's dielectric function. Afterwards, the converted light is coupled out to the drop port and detected using an optical spectrum analyzer.

In Fig. 1(a) we show the spectra of the transmitted light initially resonant with one of the ring's resonance wavelengths when the pump is off (green line) and when it is on (red line). It is seen that when the pump laser is turned on, 15 new wavelengths are generated, all of which are located at the new resonances of the ring resonator. This uniquely demonstrates that photonic transitions between different cavity modes have been realized in this silicon microcavity. The furthest mode has a wavelength blueshift of more than 8 nm from the initial wavelength. A schematic drawing of this process is shown in Figs. 1(b) and 1(c) illustrating that light is directly transitioned from the initially excited cavity mode to the 15 other modes by the dynamic tuning of the cavity's refractive index.

In order to understand the mechanism of the photonic transitions, one can follow a derivation similar to the time-dependent theory of electronic transitions in quantum mechanics, thanks to the similarity of Maxwell's equations and the Schrödinger equation, to obtain the probability amplitudes for the optical modes [16,17]:

$$i \frac{d}{dt} a_m(t) = \sum_n V_{mn}(t) a_n(t) \exp[i(\omega_m - \omega_n)t]. \quad (1)$$

Here  $a_m(t)$  is the amplitude of the  $m$ th-order cavity mode of the resonator associated with an eigenvalue of angular frequency  $\omega_m$ . Furthermore, we assume here that the perturbation of index will not modify the unperturbed cavity modes. The matrix elements  $V_{mn}(t)$  describe the coupling between different modes when a perturbation is applied on this system. These are given by [16,17]

$$V_{mn} = - \frac{\omega_n \mu}{(2\pi)^3} \int d^3\mathbf{r} \frac{\delta\epsilon(\mathbf{r}, t)}{\epsilon} \mathbf{H}_m^* \cdot \mathbf{H}_n. \quad (2)$$

Here  $\mathbf{H}_m$  is the magnetic field of the  $m$ th-order cavity mode,  $\mu$  is the permeability constant,  $\epsilon$  is the dielectric function of unperturbed system and  $\delta\epsilon(\mathbf{r}, t)$  is the time and spatial dependent perturbation of the dielectric function. We see that in order to induce photonic transitions, the spatial part of  $\delta\epsilon(\mathbf{r}, t)$  must produce a nonvanishing integral in Eq. (2). Since  $\mathbf{H}_m$  and  $\mathbf{H}_n$  are orthogonal for  $m \neq n$ , this can only be realized by a nonuniform spatial dielectric change. In order to satisfy the condition of nonuniform

spatial dielectric change, when the ring is illuminated by the pump care is taken to ensure that the spot size of the pump beam does not overlap completely with the ring. Additionally, as deduced by Eq. (1), the temporal variation of  $\delta\epsilon(\mathbf{r}, t)$  must have a nonzero Fourier component near the transition frequency (defined as  $\Delta\omega = \omega_m - \omega_n$ ). To achieve this condition, one can modulate the index at a frequency equal to  $\Delta\omega$  resulting in resonant transitions [15], which is exactly the case of comb frequency generators [12] and interband transitions in photonic crystals [16]. Alternatively, one could use an ultrafast index change where the frequency bandwidth of the time-dependent index change overlaps  $\Delta\omega$ . This condition can be approximated as  $\tau_c \sim 1/\Delta\omega$ , where  $\tau_c$  is the time to complete the index change. Here we achieve an index change in a time scale of the order of 100 fs, corresponding to the inverse of a frequency of the order of 1 THz, spanning a number of modes separated by  $\sim 100$  GHz.

In order to analyze the dynamics of the cavity and the efficiency of the process, we measure the photonic transitions using a ring resonator with a radius 50  $\mu\text{m}$  that has a larger free spectral range of 1.9 nm at wavelength around 1569 nm for quasi-TM mode. The full width at half maximum bandwidth of the resonance is 0.13 nm, which results in a quality factor  $Q = 12000$ . This quality factor corresponds to a photon lifetime of approximately 10 ps. In Fig. 2(a), we show the spectrum of the transmitted light when the pump is off and the probe wavelength is set to be on resonance. The large peak near 1567.5 is the initial mode of the cavity directly excited by the cw laser; the other peaks are a result of the background amplified spontaneous emission (ASE) of the cw laser. These peaks provide a reference for all of the initial cavity modes in the spectral range under consideration. In Fig. 2(b) the pump is turned on with pulse duration of 200 fs, however the incident light is tuned to be off-resonance with the ring resonator. Here we see no sign of conversion to new wavelengths despite the modulation of the cavity's dielectric function by the pump beam. This is due to the fact that since no resonant mode is excited by the input wavelength, there can be no transition to other states (ASE excitation of the resonances is too weak). However, as we tune the input wavelength to be on resonance with the ring, seven new wavelengths appear at the new resonances of the cavity, indicated by green arrows in Fig. 2(c). This uniquely demonstrates that all of the new wavelengths are generated by conversion of the initial probe state to the new photonic states. Note in Fig. 2(c) that the new wavelengths appear at the resonances of the perturbed ring which are slightly blue shifted from the initial states by the induced refractive index change [14]. Since the photon lifetime (10 ps) is much smaller than the carrier recombination lifetime (450 ps) the converted photons leak out from the resonator (and are measured) before the ring returns to its unperturbed state. The 0th order conversion comes from the adiabatic transition of initial mode to the perturbed mode of the same order. This adiabatic frequency conversion has

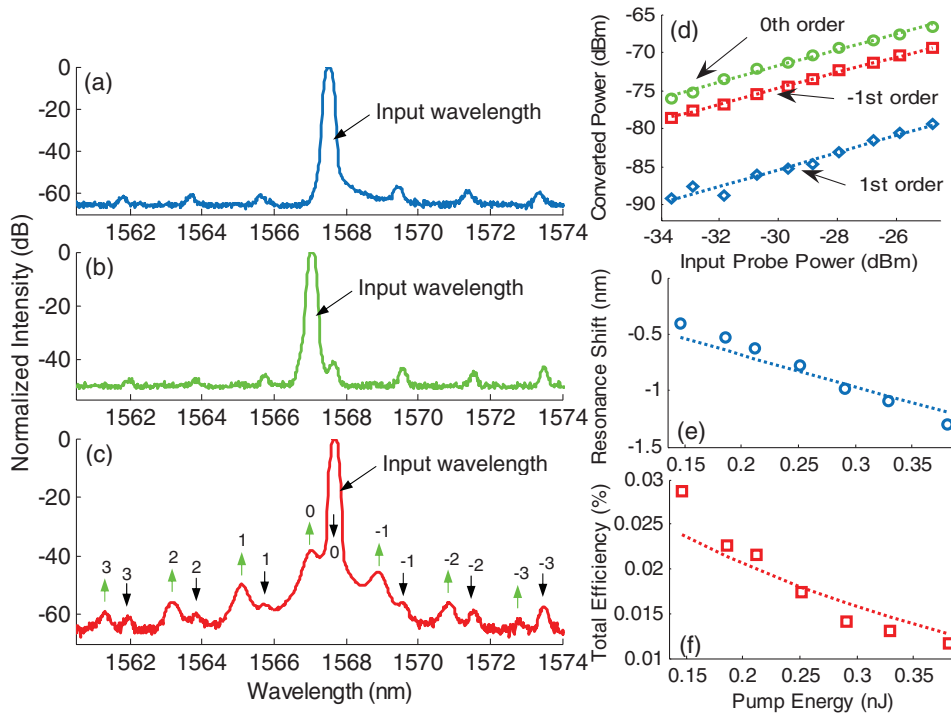


FIG. 2 (color). (a) Spectrum of the drop port. The input wavelength of the cw laser is on resonance with the ring cavity (large peak). Other resonance peaks appear, resulting from amplified spontaneous emission of the laser. (b) Spectrum of the drop port when the pump is present. The input probe wavelength is detuned from the ring resonance. (c) Same as in (b) when the input wavelength is on resonance with the ring cavity. Seven new wavelengths appear in the spectrum. The black arrows indicate the original modes and the green arrows indicate the newly generated wavelengths. (d) The amplitudes of the generated wavelengths versus the probe power. The dashed lines are linear fittings of the data. (e) The wavelength shift for the 0-order mode versus the pump energy. (f) Total conversion efficiency (the sum of all efficiency for new generated waves) versus the pump energy. In (e)–(f) the dashed lines serve as a guide to the eye.

been investigated in several references [10,11,18,19], however, its frequency shift is limited by the index change. In contrast, here the transitions between the modes of different orders do not suffer from this limitation. From Fig. 2(c), the maximum wavelength shift is  $-6.3$  nm, and the absolute conversion efficiencies for the 0th order and  $-1$ st order are 0.016% and 0.003%, respectively. These conversion efficiencies seem low because the cw probe light is only converted whenever a pump pulse occurs (every 13 ns). Taking this into account and the photon lifetime of the cavity we determine the conversion efficiency per pump pulse to be approximately 20% for the 0th order mode and 4% for the  $-1$ st order (The conversion efficiency per pump pulse can be extracted from the measured efficiency multiplied by  $T/\tau_{\text{ph}}$ , where  $T$  is the period of the pump pulses and  $\tau_{\text{ph}}$  is the photon lifetime.). In addition, we measure the effect for various probe and pump powers. The results of these measurements are shown in Figs. 2(d)–2(f). It is seen that the conversion efficiencies remain constant as we vary the probe power (the pump energy is fixed at 0.28 nJ), demonstrated by Fig. 2(d). The wavelength change varies linearly with pump power as would be expected with linear absorption of the pump. It is also seen that the total conversion efficiency decreases

with increasing pump power in Fig. 2(f) due to increased free-carrier absorption [14].

In order to verify that high-speed refractive index modulation is necessary to achieve the transitions between modes of different orders, we measure the spectrum at the drop port obtained under different pump pulse durations. The input wavelength is tuned to the initial resonance of the cavity. The pump pulse duration is varied by using a two-grating system, in which grating dispersion is introduced to temporally expand the pulse [20]. We see in Fig. 3, where the spectra for different pulse durations is shown, that the transition probabilities for  $-1$ -order and 1-order transitions increase as the pulse duration decreases. This is the case because as the pulse duration decreases the frequency bandwidth of the dynamic index change increases, allowing more efficient conversion to modes of different orders according to Eq. (1).

In conclusion, we experimentally demonstrate the generation of new frequencies by inducing photonic transitions between discrete modes of a silicon optical microcavity, in analogy to electronic transitions. In this work, the efficiency of conversion is limited by the quality factor of the micro-ring resonators used. Since the optical energy trapped in a cavity is linearly proportional to its

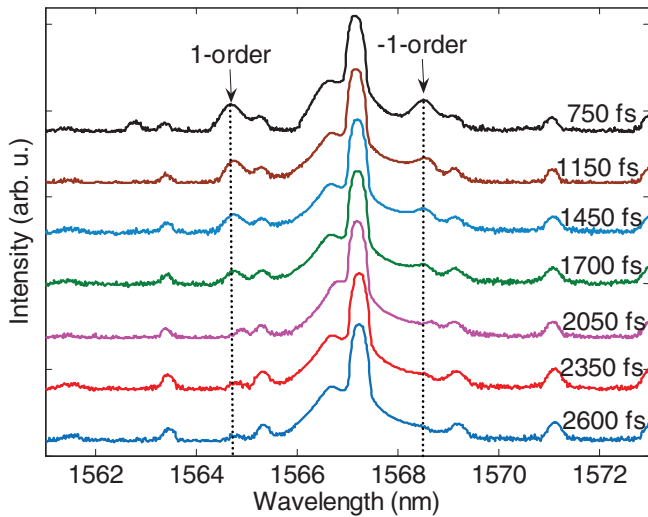


FIG. 3 (color). (a) Spectra with different pump pulse durations. It is evident that the probability of nonadiabatic transitions increase as the pulse duration becomes shorter.

quality factor, the use of other types of high-quality-factor microcavities such as photonic crystal structures and suspended micro disks or toroids [2,3] may increase the efficiency of the process. The demonstrated device allows the generation of new wavelengths of light in materials such as silicon which are generally not optically active [21,22]. In particular, a miniaturized optical comb source on silicon could revolutionize optical communications, optical interconnects for high performance computing, optical sensing and lab-on-chip devices. In recent years, a coherent light source on silicon has been intensively sought, however until today, only narrow band sources based on nonlinear effects such as Raman, requiring high power pump sources, have been successfully demonstrated [21]. Note that in order to ensure that the device can be used as on-chip optical sources, a compact pump is required. We have recently demonstrated that using carrier plasma dispersion effect one can alter the refractive index of silicon with ultrafast time response ( $\sim 50$  ps) by a forward PIN structure [23]. As the saturated speed of free carriers in silicon is  $\sim 10^7$  cm/sec [24], one can fundamentally achieve  $\sim 1$  ps transition time for a  $0.1 \mu\text{m}$  depletion length in a ring resonator. This can be used to demonstrate electrically pumped comb sources with the overall bandwidth of a few nm. In addition, in recent years, mode-locked semiconductor lasers have been successfully demonstrated with a pulse duration in the order of 100 fs [25–27]. This would enable on-demand hybrid integrated silicon comb sources distributed on chips using a single external and compact light source as pump.

The authors acknowledge support by the Center for Nanoscale Systems, supported by the National Science Foundation. We thank Gernot Pomrenke from the Air Force Office of Scientific Research (AFOSR) for partially

supporting this work. This work was performed in part at the Cornell Nano-Scale Science & Technology Facility (a member of the National Nanofabrication Users Network) which is supported by National Science Foundation. P. D. would also like to acknowledge additional support from the NSERC of Canada.

\*Author to whom correspondence should be addressed.  
ml292@cornell.edu

- [1] J. D. Joannopoulos, P. R. Villeneuve, and S. H. Fan, *Nature (London)* **386**, 143 (1997).
- [2] K. J. Vahala, *Nature (London)* **424**, 839 (2003).
- [3] Y. Akahane, T. Asano, B. S. Song, and S. Noda, *Nature (London)* **425**, 944 (2003).
- [4] B. Julsgaard, J. Sherson, J.-I. Cirac, J. Fiurásek, and E. S. Polzik, *Nature (London)* **432**, 482 (2004).
- [5] O. Painter *et al.*, *Science* **284**, 1819 (1999).
- [6] H. G. Park *et al.*, *Science* **305**, 1444 (2004).
- [7] M. Soljacic and J. D. Joannopoulos, *Nat. Mater.* **3**, 211 (2004).
- [8] M. F. Yanik and S. H. Fan, *Phys. Rev. Lett.* **92**, 083901 (2004).
- [9] Q. Xu, P. Dong, and M. Lipson, *Nature Phys.* **3**, 406 (2007).
- [10] E. J. Reed, M. Soljacic, and J. D. Joannopoulos, *Phys. Rev. Lett.* **90**, 203904 (2003).
- [11] S. F. Preble, Q. Xu, and M. Lipson, *Nat. Photon.* **1**, 293 (2007).
- [12] T. Kobayashi, T. Sueta, Y. Cho, and Y. Matsuo, *Appl. Phys. Lett.* **21**, 341 (1972).
- [13] A. Yariv, *Optical Electronics in Modern Communications* (Oxford University, New York, 1997).
- [14] R. A. Soref and B. R. Bennett, *IEEE J. Quantum Electron.* **23**, 123 (1987).
- [15] V. R. Almeida *et al.*, *Opt. Lett.* **29**, 2867 (2004).
- [16] J. N. Winn, S. H. Fan, J. D. Joannopoulos, and E. P. Ippen, *Phys. Rev. B* **59**, 1551 (1999).
- [17] N. Malkova, S. Kim, and V. Gopalan, *Phys. Rev. B* **68**, 045105 (2003).
- [18] M. Notomi and S. Mitsugi, *Phys. Rev. A* **73**, 051803 (2006).
- [19] M. Notomi, H. Taniyama, S. Mitsugi, and E. Kuramochi, *Phys. Rev. Lett.* **97**, 023903 (2006).
- [20] E. B. Treacy, *IEEE J. Quantum Electron.* **5**, 454 (1969).
- [21] H. Rong *et al.*, *Nature (London)* **433**, 292 (2005).
- [22] M. A. Foster *et al.*, *Nature (London)* **441**, 960 (2006).
- [23] Q. Xu, S. Manipatruni, B. Schmidt, J. Shakya, and M. Lipson, *Opt. Express* **15**, 430 (2007).
- [24] C. M. Wolfe, N. Holonyak, and G. E. Stillman, *Physics Properties of Semiconductors* (Prentice Hall, Englewood Cliffs, NJ, 1989), Chap. 5, p. 165.
- [25] P. Vasil'ev, *Ultrafast Diode Lasers: Fundamentals and Applications* (Artech House, Boston, 1995), Chap. 4, p. 95.
- [26] E. A. Avrutin, J. H. Marsh, and E. L. Portnoi, *IEE Proc. Optoelectronics* **147**, 251 (2000).
- [27] E. U. Rafailov, M. A. Cataluna, and W. Sibbett, *Nat. Photon.* **1**, 395 (2007).